

ROTATIONAL INDUCTION HEATING OF NONMAGNETIC CYLINDRICAL BILLETS

ING. MARTINA DONÁTOVÁ
ING. PAVEL KARBAN, PHD

Abstract: Induction heating of long cylindrical nonmagnetic billets rotating in time invariable magnetic field is modelled by integral approach. The model also includes the mechanical transient. The methodology is illustrated by an example whose results are discussed.

Key words: Induction heating, integral approach, electromagnetic field, temperature field, numerical analysis.

INTRODUCTION

Induction heating of nonmagnetic billets represents an industrial technology employed mainly for their softening before next heat treatments (such as hot forming). The classical process consisting in heating of a workpiece in an inductor is simple, but its efficiency is rather low (usually it does not exceed about 60%). That is why novel, more effective ways are looked for. For long cylindrical workpieces an efficient technique was recently introduced based on their rotation in a time invariable magnetic field produced by appropriately arranged field coils carrying DC currents (Fig. 1). For the sake of optimizing the arrangement of the system, the steady-state part of the process was analyzed by the finite element method (FEM) [1], [2].

The paper deals with an alternative way of mathematical and computer modeling of the process. The authors developed a novel method of mapping eddy currents in the system using an integrodifferential approach. Numerical solution of the corresponding mathematical model directly provides temporal and spatial distribution of eddy currents in the heated cylinder (thus, without any need to calculate the distribution of the field quantities), which substantially reduces the time of computation and numerical errors. There is also no need to care for the boundary conditions because they are implemented directly in the kernel function of the corresponding integrals. Another advantage is no need to remesh the definition area at every time step.

The next step is mapping of the temperature rise of the cylinder. This problem is solved in the quasi-coupled formulation, the electrical conductivity of the billet is

assumed to be a function of temperature. Respected is also the mechanical transient characterized by the gradual increase of revolutions up to their nominal value.

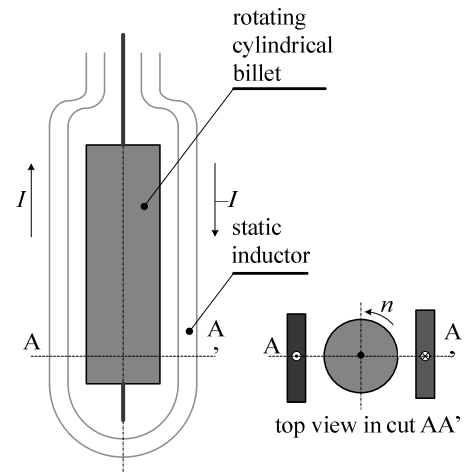


Fig. 1. Induction heating of rotating cylinder in time invariable magnetic field

1. FORMULATION OF THE PROBLEM

The top view of the solved arrangement is depicted (with principal dimensions) in Fig. 2. The arrangement is supposed to be sufficiently long in the direction of the z -axis, so that the investigated domain may be considered two-dimensional in Cartesian coordinates x, y .

The aim of the analysis is to assemble the complete mathematical model of the process and solve it numerically for the prescribed input data.

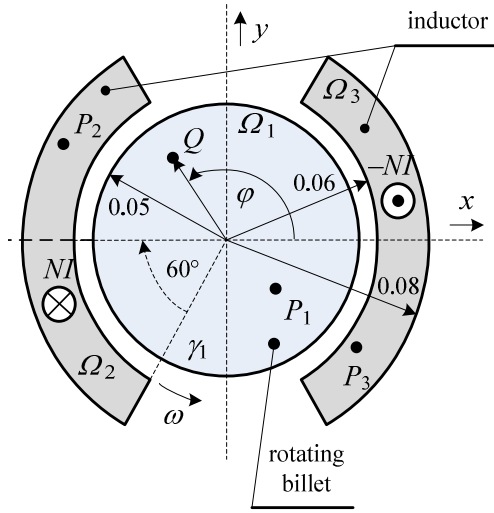


Fig. 2. Detailed top view of the solved arrangement

2. MATHEMATICAL MODEL

The mathematical model consists of the following equations and expressions:

- Integrodifferential equation describing the spatial and temporal distribution of eddy currents in the billet.
- Expression for the drag torque produced by the interaction between the time invariable magnetic field and eddy currents generated in the rotating billet.
- Partial differential equation describing the heat transfer in the system.
- Ordinary differential equation for the time evolution of the angular velocity of the billet.

Particular aspects of the model will shortly be described in the following text. For other details see [3] and [4].

Eddy currents in the heated cylinder

Consider a system containing n nonferromagnetic metal bodies Ω_j , $j=1, \dots, n$ (see Fig. 3) whose electrical conductivities are γ_j , $j=1, \dots, n$. The bodies carry currents $i_j(t)$, $j=1, \dots, n$ and each of them can move at a velocity v_j , $j=1, \dots, n$. Consider now a reference point $Q_j(\mathbf{r}_j) \in \Omega_j$ with the position vector $\mathbf{r}_j = \mathbf{r}_j(t)$.

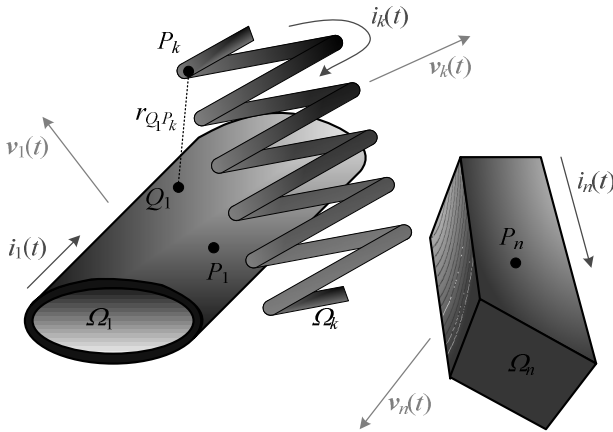


Fig. 3. A system with n electrically conductive current carrying bodies with motion

Ref. [3] contains the complete derivation of the current densities induced in the system. It can be shown that current density at a reference point $Q_j(\mathbf{r}_j) \in \Omega_j$ obeys the integrodifferential equation

$$\mathbf{J}_j(Q_j, t) + \frac{\mu_0 \gamma_j}{4\pi} \cdot \frac{d}{dt} \sum_{i=1}^n \int_{\Omega_i} \frac{\mathbf{J}_i(P_i, t) \cdot dV}{r_{P_i Q_j}(t)} + \mathbf{J}_{j0}(t) = 0, \quad j=1, \dots, n, \quad (1)$$

where, $\mathbf{J}_i(P_i, t)$ denotes the vector of total current density at a general integration point $P_i \in \Omega_i$ at time t , $r_{P_i Q_j}(t)$ is the distance between the reference point Q_j and point of integration P_i (for an illustration, Fig. 3 depicts such a distance between points Q_1 and P_k) and $\mathbf{J}_{j0}(t)$ is an unknown time function. This function must be determined indirectly from the condition of the total current that reads

$$\iint_{S_j} \mathbf{J}_j(Q_j, t) dS = i_j(t), \quad (2)$$

where S_j denotes the corresponding cross section. This relation is applied in such elements where the total current $i_j(t)$ is known.

Equation (1) may further be modified as follows:

$$\mathbf{J}_j(Q_j, t) + \frac{\mu_0 \gamma_j}{4\pi} \cdot \sum_{i=1}^n \int_{\Omega_i} \frac{d\mathbf{J}_i(P_i, t) \cdot dV}{dt \cdot r_{P_i Q_j}(t)} - \frac{\mu_0 \gamma_j}{4\pi} \cdot \sum_{i=1}^n \int_{\Omega_i} \frac{(\mathbf{v}_{ij}(t) \cdot \mathbf{r}_{P_i Q_j}(t)) \mathbf{J}_i(P_i, t) dV}{r_{P_i Q_j}^3(t)} + \mathbf{J}_{j0}(t) = 0, \quad j=1, \dots, n, \quad (3)$$

where $\mathbf{v}_{ij}(t) = \mathbf{v}_i(t) - \mathbf{v}_j(t)$, $\mathbf{r}_{P_i Q_j}(t) = \mathbf{r}_{P_i}(t) - \mathbf{r}_{Q_j}(t)$. The second term on the left-hand side denotes the component of eddy currents due to transformation and the third one another component due to motion.

Now equation (3) will be modified for the arrangement in Fig. 2 that is supposed sufficiently long in the axial direction. In such a case the arrangement has 2D feature and its solution can be performed in the polar coordinate system. Distribution of current densities having the only component in the z -direction is then given by equation

$$J_{1z}(r, \varphi) = \frac{\mu_0 \omega \gamma_1}{2\pi} \cdot \frac{d}{d\varphi} \int_{\Omega_1} J_{1z}(P_1) \ln(s_{QP_1}) dS + \frac{\mu_0 \omega \gamma_1 J_{2z}}{2\pi} \cdot \frac{d}{d\varphi} \int_{\Omega_2} \ln(s_{QP_2}) dS + \frac{\mu_0 \omega \gamma_1 J_{3z}}{2\pi} \cdot \frac{d}{d\varphi} \int_{\Omega_3} \ln(s_{QP_3}) dS, \quad (4)$$

where γ_1 is the electrical conductivity of the billet, s_{QP_1} , s_{QP_2} , and s_{QP_3} are the distances between the reference point Q (φ denoting its angle with respect to the x -axis), and general integration points P_1 , P_2 , and P_3 in regions Ω_1 (billet), Ω_2 , and Ω_3 (left and right parts of

the field coil), respectively. Finally $J_{2z} = -J_{3z}$ is the current density in the field coil calculated from the current I and cross section of the coil (this density is considered independent of the eddy currents produced in the billet).

Specific Joule losses in the heated cylinder

Knowledge of the specific Joule losses w_j in the j th body in Fig. 3 is the principal condition for the consequent thermal computations. There holds

$$w_{j,j}(Q_j, t) = \frac{|J_j(Q_j, t)|^2}{\gamma_j}. \quad (5)$$

This expression can be, without any change, directly applied to the heated cylinder.

Temperature distribution in the heated cylinder

Nonstationary temperature field T in the current carrying parts of the system is described by the heat transfer equation in the form respecting the motion

$$\begin{aligned} \operatorname{div}(\lambda \operatorname{grad} T) &= \rho c_p \frac{dT}{dt} - w_j \\ &= \rho c_p \left(\frac{\partial T}{\partial t} + \mathbf{v} \cdot \operatorname{grad} T \right) - w_j, \end{aligned} \quad (6)$$

where λ is the thermal conductivity, ρ denotes the specific mass, c_p is the specific heat at the constant pressure, symbol \mathbf{v} stands for the velocity, and w_j denotes the specific Joule losses. The physical parameters of materials λ , ρ , and c_p are generally temperature-dependent functions.

Equation (6) has to be supplemented by the boundary conditions that respect the convection and radiation of heat from the body.

$$-\lambda \frac{dT}{dn} = \alpha(T - T_0) + \sigma C(T^4 - T_i^4), \quad (7)$$

where α is the convective heat transfer coefficient (that is a function of temperature and also frequency of rotation), T is the local surface temperature of the billet, σ stands for the Stefan-Boltzmann constant ($\sigma = 5.6704 \cdot 10^{-8} \text{ kg s}^{-3} \text{ K}^{-4}$), C is a constant respecting influences of emissivity, absorption and configuration factors, T_i (simplified) the temperature of the field winding and T_0 the temperature of ambient medium (air).

Mechanical transient

The billet is rotated by an asynchronous motor of given torque characteristic $T(\omega)$, where ω denotes the angular frequency. The equation describing the time evolution of ω reads

$$J \frac{d\omega}{dt} + D\omega = T(\omega) - T_d(\omega), \quad \omega(0) = 0, \quad (8)$$

where J denotes the moment of inertia of the billet, D is the coefficient of damping and $T_d(\omega)$ the strongly nonlinear drag torque due to Lorentz forces acting be-

tween the primary magnetic field and eddy currents produced in the billet.

Drag torque

The drag torque $T_d(\omega)$ will be determined not for a general arrangement, but just for the rotating billet depicted in Fig. 2. First we calculate the elementary force (per unit length) acting at point Q . Let point Q be described by coordinates r, φ (or coordinates $x = r \cos \varphi$, $y = r \sin \varphi$), while points P_2 and P_3 by coordinates x_2, y_2 and x_3, y_3 , respectively. Now the elementary force $d\mathbf{f}_{LQ}$ acting at point Q of the billet follows from expression

$$d\mathbf{f}_{LQ} = \mathbf{J}_Q \times d\mathbf{B}_Q, \quad (9)$$

where \mathbf{J}_Q is the vector of current density at point Q (as previously said, it has only one nonzero component in the z direction) and $d\mathbf{B}_Q$ is magnetic field produced by filaments located at points P_2 and P_3 of both parts Ω_2 and Ω_3 of the inductor. The vector equation (9) may be divided into two component equations

$$df_{LQx} = -J_{Qz} \cdot dB_{Qy}, \quad df_{LQy} = J_{Qz} \cdot dB_{Qx}. \quad (10)$$

The x and y components of magnetic flux density $d\mathbf{B}_Q$ at point Q due to current density at point $P_2 \in \Omega_2$ are given by formulas

$$\begin{aligned} dB_{Qx} &= -\frac{\mu_0 J_2}{2\pi} \cdot \frac{y - y_2}{(x - x_2)^2 + (y - y_2)^2}, \\ &= -\frac{\mu_0 J_2}{2\pi} \cdot \frac{r \cos \varphi - y_2}{(r \sin \varphi - x_2)^2 + (r \cos \varphi - y_2)^2}, \\ dB_{Qy} &= \frac{\mu_0 J_2}{2\pi} \cdot \frac{x - x_2}{(x - x_2)^2 + (y - y_2)^2} \\ &= \frac{\mu_0 J_2}{2\pi} \cdot \frac{r \sin \varphi - x_2}{(r \sin \varphi - x_2)^2 + (r \cos \varphi - y_2)^2} \end{aligned} \quad (10)$$

and analogous formulas can be obtained for the contributions due to current density at point $P_3 \in \Omega_3$.

The components of the total local force per unit length \mathbf{f}'_{LQ} can be obtained by integration of (10) over the cross sections S_2 and S_3

$$\begin{aligned} f'_{LQx} &= -\int_{S_2} J_{Qz} \cdot dB_{Qy} dS_2, \\ f'_{LQy} &= \int_{S_2} J_{Qz} \cdot dB_{Qx} dS_2. \end{aligned} \quad (11)$$

The elementary torque t_Q acting at point Q is now given by formula

$$t_Q = \mathbf{r} \times \mathbf{f}_Q \quad (12)$$

has only one nonzero component in the direction of the z -axis

$$t_{Qz} = x \cdot f_{Qy} - y \cdot f_{Qx}. \quad (13)$$

The total torque $T'_d(\omega)$ per unit length is given by integration of t_{Qz} over Ω_1 . The total torque is then obtained

by multiplying $T_d'(\omega)$ by the length of the billet (with some error due to disregarding the front effects).

3. NUMERICAL SOLUTION OF THE MODEL

The model was solved by a code developed and written by the authors. The integrodifferential model of eddy currents was solved by a technique similar to the finite elements. The definition area was discretized by a triangular mesh, the distribution of eddy currents in particular cells of the heated billet was replaced by an appropriate function and their time evolution was solved by the Runge–Kutta method. The nonstationary temperature field (6) was solved by the classical finite element method of the first order that is well known, so that no details will be provided in the paper. As for the movement equation (8), it was also solved by the Runge–Kutta method, where at each time level the drag torque $T_d(\omega)$ was recalculated appropriately.

Particular attention was paid to the convergence of results depending on the density of the discretization mesh and time step. As the integrodifferential method works with dense matrices, the highest number of elements in the mesh could not exceed about 10000.

4. ILLUSTRATIVE EXAMPLE

For an illustration, we analyzed in details the process of heating of an aluminum billet. The basic geometry of the arrangement is shown in Fig. 2. Other principal data follow:

- axial length of the billet $l = 0.3$ m,
- mass of the billet $m = 6.362$ kg,
- moment of inertia of the billet $J = 0.00795$ kgm²,
- field current density $J_{2z} = 2.7285 \times 10^7$ A/m²,
- coefficient of damping $D = 0.001$ kgm²/s,
- torque of the induction motor driving the billet $T(\omega) = 410$ Nm,
- maximum revolutions $n_{\max} = 2850$ /min,
- number of coils 1–4 (but the total magnetomotive force remaining the same, as well as the surface of their cross-section).

The computations provided a lot of results. Fig. 4 shows the distribution of the module of current densities in the arrangement with one field coil and Fig. 5 in the arrangement with four field coils.

Fig. 6 shows the distribution of the specific Joule losses in the steady state (at the maximum revolutions of the drive) produced along the radius of the billet for various radii. It is clear that these losses are produced just in the surface layer of the billet, whose thickness is about 0.015 m (which well corresponds with the depth of penetration).

Although the specific Joule losses produced along the radii in Fig. 6 differ from one another (some of them very much), for further computations we can consider their average values during one revolution. The dependence of the average Joule losses w_{Ja} along the radius of the billet is shown in Fig. 7. Even this figure confirms the above conclusion, that is, the specific Joule losses are produced

in the layer of thickness corresponding to the depth of penetration.

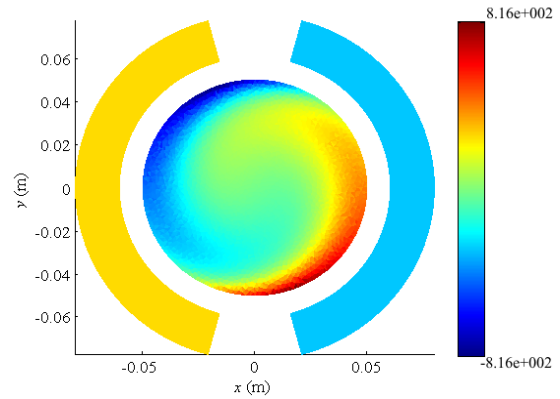


Fig. 4. Distribution of current density in a system with one field coil

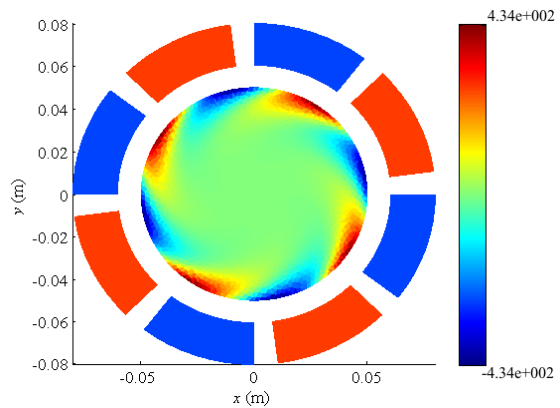


Fig. 5. Distribution of current density in a system with four field coils

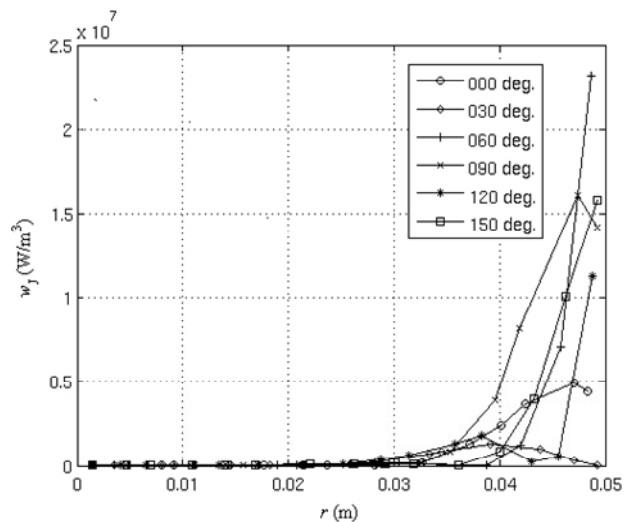
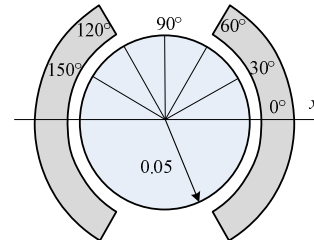


Fig. 6. Distribution of the specific Joule losses along the radius of the billet for various angles

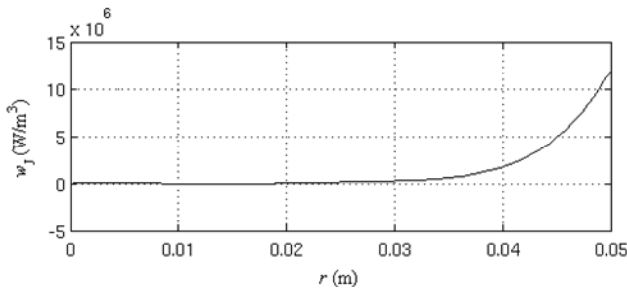


Fig. 7. Distribution of the average specific Joule losses along the radius of the billet (one field coil)

Fig. 8 shows the dependence of the drag torque of the billet as a function of revolution for varying number of the field coils. The shapes of the characteristics remind of the torque characteristic of an asynchronous machine.

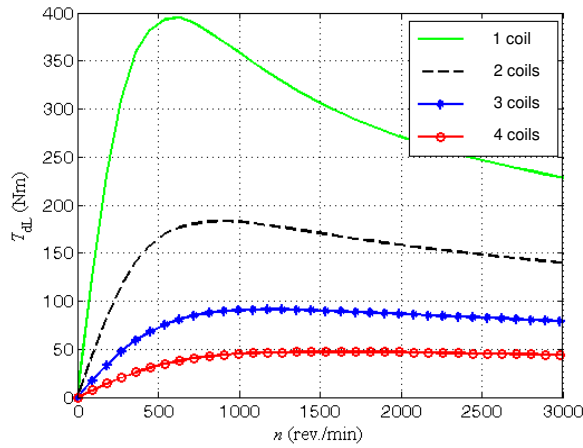


Fig. 8. Dependence of the drag torque on revolutions for various numbers of the field coils

Fig. 9 depicts the dependence of revolutions on time for varying number of the field coils. It is obvious that even in the most unfavorable case the time of reaching steady state (for one field coil) does not take more than 0.04 s.

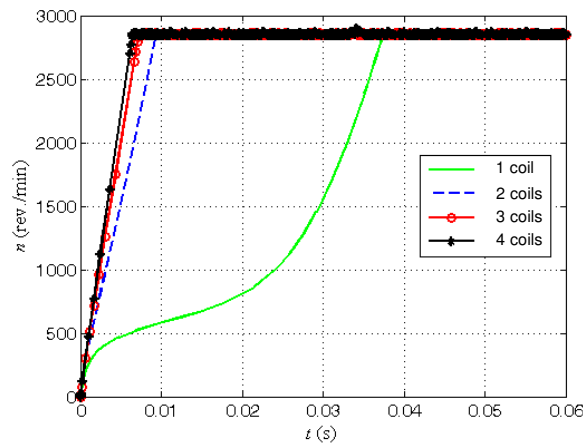


Fig. 9. Revolutions of the billet as a function of time for various numbers of the field coils

The last Fig. 10 shows the time evolution of the average temperature of the billet. The dependence is practically linear.

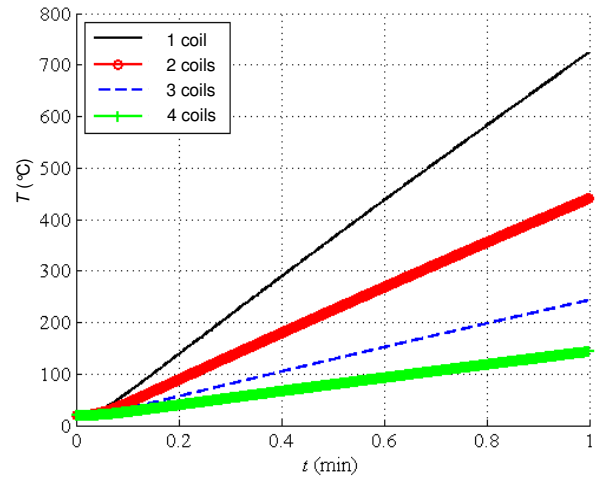


Fig. 10. Time evolution of the average temperature of the billet as a function of the number of the field coils.

It is obvious that the variant with one coil is the best one (this corresponds with Fig. 4, the modules of the eddy current density over the cross-section of the billet reach the highest values in this case).

5. CONCLUSION

The methodology of solution is correct and sufficiently fast (the computations take minutes or tens of minutes). Some results of calculations were compared with data obtained using professional codes (COMSOL Multiphysics). The accordance was very good (the differences between the results did not exceed about 5%). The future work in the domain will be aimed at the acceleration of the suggested algorithm and evaluation of the inverse possibility of induction heating of an unmoving billet by rotating coils or permanent magnets.

REFERENCES

- [1] M. Zlobina, B. Nacke, and A. Nikonarov: Electromagnetic and Thermal Analysis of Induction Heating of Billets by Rotation in DC Magnetic Field. Proc. UIE Krakow, Poland, May 2008, pp. 21–22.
- [2] S. Lupi and M. Forzan: A Promising High Efficiency Technology for the Induction Heating of Aluminium Billets. Proc. UIE Krakow, Poland, May 2008, pp. 19–20.
- [3] P. Karban, I. Dolezel, and P. Solin: Computation of General Nonstationary 2D Eddy Currents in Linear Moving Arrangements Using Integrodifferential Approach. COMPEL, Vol. 25, 2006, No. 3, pp. 635–641.
- [4] P. Karban, I. Dolezel, and M. Donatova: Integrodifferential Approach to Modeling of Continual Induction Heating of Nonmagnetic Cylindrical Bodies. Acta Technica CSAV 53, No. 2, pp. 173–192.

Authors: Ing. Martina Donátová, Ing. Pavel Karban, PhD., University of West Bohemia, Faculty of Electrical Engineering, Univerzitni 26, 306 14 Pilsen, CR, E-mail: {mdonat, karban}@kte.zcu.cz.